Eur. Phys. J. D **14**, 377–386 (2001)

THE EUROPEAN PHYSICAL JOURNAL D

EDP Sciences

Preparation and decoherence of superpositions of electromagnetic field states

H.-P. Breuer[1,a], U. Dorner[1], and F. Petruccione[1,2]

[1] Albert-Ludwigs-Universität, Fakultät für Physik, Hermann-Herder-Straße 3, 79104 Freiburg im Breisgau, Germany
[2] Istituto Italiano per gli Studi Filosofici, Palazzo Serra di Cassano, Via Monte di Dio 14, 80132 Napoli, Italy

Received 13 September 2000 and Received in final form 22 December 2000

Abstract. In a recent experiment the progressive decoherence of a mesoscopic superposition of two coherent field states in a high-Q cavity, known as Schrödinger cat state, has been measured for the first time [Brune *et al.*, Phys. Rev. Lett. **77**, 4887 (1996)]. Here, the full master equation governing the coupled dissipative dynamics of the atom-field system studied in the experiment is formulated and solved numerically for the experimental parameters. The model simulated avoids the approximations underlying an analytically solvable model which is based on a harmonic expansion of the energies of the dressed atomic states and on a treatment of their dynamics within the adiabatic approximation. In particular, the numerical simulations reveal that the coupling of the cavity field mode to its environment causes important decoherence effects already during the initial preparation phase of the Schrödinger cat state. This phenomenon is investigated in detail with the help of a measure for the purity of states. Moreover, the Hilbert-Schmidt distance of the intended target state, the Schrödinger cat, to the state that is actually prepared in the experiment is determined.

PACS. 32.80.-t Photon interactions with atoms – 03.65.Ta Foundations of quantum mechanics; measurement theory – 42.50.-p Quantum optics

1 Introduction

The emergence of classical behaviour is one of the most fundamental problems in quantum mechanics. In principle, due to its linear structure quantum mechanics allows the existence of superpositions of macroscopically distinguishable states which would arise, *e.g.*, in measurement-like processes as a direct consequence of the unitary Schrödinger dynamics. However, such states are (of course) never observed. Schrödinger himself emphasized this problem in his famous Gedankenexperiment of a simultaneously dead and alive cat [1].

A well-established approach to the decoherence problem is based on the idea that a macroscopic system, like a measurement device, is never isolated from its environment [2,3]. Taking this as a starting point one can derive an equation of motion, *e.g.* for the reduced density operator, which describes the dynamics of the system under consideration. In general, these equations lead to a non-unitary evolution of the density operator and it has been shown in a variety of examples how classical properties can emerge in such situations (see [2] and references therein).

In addition to these theoretical considerations, great experimental progress has been achieved in the last few years in order to enlighten the phenomenon of decoherence. For example, it was possible to prepare a superposition of two motional states of the center of mass coordinate of a Be^+ ion stored in the harmonic potential of a Paul-trap [4] and to measure its decoherence [5]. Another famous experiment, lying in the domain of cavity quantum electrodynamics, creates a superposition of two (mesoscopic) coherent field states in a superconducting microwave cavity [6]. In this experiment the progressive decoherence of such a Schrödinger cat-type state has been observed for the first time.

In theoretical and experimental considerations it is sometimes assumed that a mesoscopic or macroscopic superposition is prepared and that *then* the coupling of the system to its environment destroys the coherence of the superposition. This is of course an idealization. Even if the preparation time is very small one has to pay attention to the fact that decoherence time scales are mostly extremely small, too (see, *e.g.* [7–9]). In more realistic treatments the coupling of a system to its environment is taken into account already during the preparation process [10–14].

Following this idea, the subject of the present work is the examination of decoherence effects during the preparation process by means of the example of the above mentioned experiment [6]. In this experiment a first atom, prepared in a superposition of two circular Rydberg states, interacts non-resonantly with the mesoscopic microwave field in a high-Q cavity leading to an (entangled) superposition of two coherent field states with different phase. One can interpret this process as an emulation of an ideal measurement in which coherent field states with different phases act as (mesoscopic) pointer states indicating the

[a] e-mail: breuer@physik.uni-freiburg.de

state of a microscopic object (the atom). If the measured object is in a superposition, this superposition is transfered to the measurement apparatus the state of which becomes a Schrödinger cat of different pointer states. Due to the interaction of the apparatus with its environment this state will decohere on a small time scale. Information about the progress of this decoherence is then gained by a second "probe" atom which crosses the apparatus after a variable delay time and which is, like the first atom, finally measured in two field ionisation detectors.

In this paper we investigate the decoherence during the preparation process of the experiment with the help of the complete quantum Markovian master equation that governs the coupled atom-field dynamics. In reference [6] the experimental data were compared with the theoretical predictions of a simplified analytical model which involves several approximations. These approximations are not necessary within our model. Especially, the coupling of the field to the environment during the interaction of field and atom can be taken into account. However, it is no longer possible to solve the equations of motion analytically. We therefore solve the full master equation numerically. These simulations allow a detailed look at the nascency of the Schrödinger cat state. It turns out that decoherence takes place already during the preparation (*i.e.*, during the measurement process) of the mesoscopic superposition in an appreciable way although the interaction time of atom and field is small and the coupling of the field to the environment is weak. In a way, this is not surprising since decoherence time scales are often much smaller than relaxation time scales.

This article is structured as follows. In Section 2 we give a short description of the experiment. Section 3.1 presents the model which is used to perform the numerical calculations and Section 3.2 briefly reviews the approximative model which leads to an analytical description of the systems dynamics. In particular, we discuss the conditions which allow the application of this model. In Section 4 we present and discuss the results of numerical simulations using the Wigner function and a measure for the purity and for the distance of states. Furthermore the quantity which was actually measured in the experiment is presented.

2 A brief description of the experiment

In this section we give a short review of the experiment of Brune *et al.* [6]. For more technical details see also [15].

Rubidium atoms are excited into a circular Rydberg state (denoted here as $|e\rangle$) with principal quantum number $n = 51$ by a pulsed process and cross a sequence of resonators R_1, C and R_2 (see Fig. 1). Ideally, only one atom with an approximately sharp defined center of mass velocity ($v = 400\,\mathrm{m/s}$) is prepared in this state and also the position r of the Rydberg atoms is suitably well-defined such that it is possible to speak of single Rydberg atoms crossing the setup. A pair of such pulses is generated with a separation ranging from $30\,\mu$s to $250\,\mu$s. Within the experiment there is also a second, lower lying Rydberg state

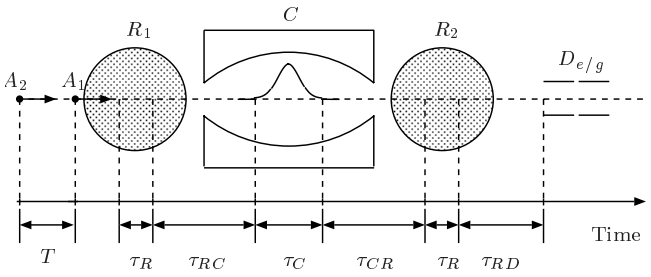

Fig. 1. Schematic setup of the experiment performed by Brune *et al.* The atoms A_1 and A_2 move along the dashed horizontal line with a time delay T and cross the resonators R_1, C, R_2 and detectors D_e and D_g. The times of flight between and within the different components are also indicated.

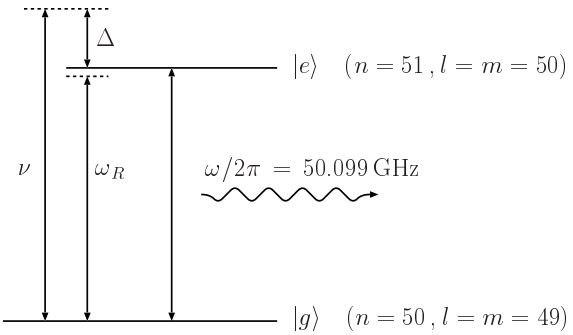

Fig. 2. Two level scheme displaying the atomic transition frequency ω, the frequency ν of the field in the Fabry-Pérot cavity C and the frequency ω_R of the fields in the resonators R_1 and R_2. The frequency ν is detuned by an amount Δ from the atomic frequency ω.

$|g\rangle$ with principal quantum number $n = 50$. These states have a very long radiative lifetime ($\gamma_\mathrm{at}^{-1} = 30\,\mathrm{ms}$), much longer than the time an atom needs to cross the whole setup ($\approx 500\,\mu$s) and a very strong coupling to radiation. The internal degrees of freedom can therefore be described as an atomic two level system (see Fig. 2) with a transition frequency in the microwave domain ($\omega/2\pi = 50.099\,\mathrm{kHz}$).

The resonators R_1 and R_2, which constitute the experimental setup of the Ramsey method of separated oscillating fields [16], contain a classical microwave field. The field strength is chosen in such a way that the atoms undergo a $\pi/2$-pulse while crossing these resonators. The high-Q Fabry-Pérot cavity C, which stores a small coherent field $|\alpha\rangle$ is made up of two superconducting niobium mirrors leading to a mean photon lifetime of $T_\mathrm{R} = 160\,\mu$s. The geometry of the relevant TEM_{900}-mode provides a smooth variation of the coupling between an atom and the field,

$$\Omega(r) = \Omega_0 \exp\left[-\frac{r^2}{w_0^2}\right], \tag{1}$$

along the beam axis with a mode waist $w_0 = 5.9\,\mathrm{mm}$ and maximum coupling $\Omega_0/2\pi = 24\,\mathrm{kHz}$ at cavity center. The cavity C is slightly detuned by an amount $\Delta = \omega - \nu$ from the atomic transition frequency. After passing the resonators the internal states of the atoms are detected by two field ionisation detectors D_e and D_g.

As we will see in the next section the first one of a pair of atoms prepares a superposition of two mesoscopic field states. This state will decohere on a very small time scale. The progress of the decoherence is read out (after a variable delay time T) by the second atom through measurement of the quantity

$$\eta = W_{\rm ee} - W_{\rm ge}. \tag{2}$$

Here, $W_{\rm ge}$ is the probability of measuring the second atom in the state $|e\rangle$ under the condition that the first one was detected in $|g\rangle$, while $W_{\rm ee}$ is the probability of measuring the second atom in the state $|e\rangle$ under the condition that the first atom was found in $|e\rangle$. Within an approximative model the information in which the first atom was measured is stored only in the off-diagonal elements of the superposition's density matrix. If they vanish, the quantity η vanishes on the same time scale.

3 The model

Let us now develop the theoretical description of the dynamics of the experimental system. To this end, we introduce an exact model which is the basis of the numerical calculations performed in Section 4. The relation to an approximative model which permits an analytical description of the systems dynamics will also be discussed.

3.1 The full master equation for the atom-field system

The total Hilbert space of the system takes the form

$$\mathcal{H} = \mathcal{H}_{\rm A_1} \otimes \mathcal{H}_{\rm A_2} \otimes \mathcal{H}_{\rm F} \otimes \mathcal{H}_{\rm B}, \tag{3}$$

where $\mathcal{H}_{\rm A_1}$ and $\mathcal{H}_{\rm A_2}$ are associated with the internal degrees of freedom of the atoms, $\mathcal{H}_{\rm F}$ is the Hilbert space of the field in the cavity C, and $\mathcal{H}_{\rm B}$ describes the environment which interacts with the field leading to the effect of decoherence. As we already noticed, spontaneous emissions of the atoms may be neglected here since the decay time is about 30 ms which is much larger than any other time scale in the experiment.

The quantum Markovian master equation which describes the interaction of an atom and the field in the central cavity takes the following form in the interaction picture

$$\dot\rho_{\rm 12F}(t) = -\frac{\rm i}{\hbar}\left[H_{\rm 12F}(t), \rho_{\rm 12F}(t)\right] + \mathcal{L}_{\rm F}\rho_{\rm 12F}(t), \tag{4}$$

where $\rho_{\rm 12F}$ denotes the density operator of atom 1, atom 2 and the radiation field in the cavity C. The superoperator $\mathcal{L}_{\rm F}$ is given by

$$\mathcal{L}_{\rm F}\rho_{\rm 12F} = \gamma\Big(b\rho_{\rm 12F}b^\dagger - \frac{1}{2}b^\dagger b\rho_{\rm 12F} - \frac{1}{2}\rho_{\rm 12F}b^\dagger b\Big) \tag{5}$$

with relaxation rate $\gamma = 1/T_{\rm R}$ and the coherent part of equation (4) is described by the Jaynes-Cummings type Hamiltonian

$$\begin{aligned} H_{\rm 12F}(t) = {}& \hbar\Omega(t)\big({\rm e}^{{\rm i}\Delta t}{\rm e}^{{\rm i}\lambda_1}b\sigma_1^\dagger + {\rm e}^{-{\rm i}\Delta t}{\rm e}^{-{\rm i}\lambda_1}b^\dagger\sigma_1\big) \\ & + \hbar\Omega(t-T)\big({\rm e}^{{\rm i}\Delta t}{\rm e}^{{\rm i}\lambda_2}b\sigma_2^\dagger + {\rm e}^{-{\rm i}\Delta t}{\rm e}^{-{\rm i}\lambda_2}b^\dagger\sigma_2\big). \end{aligned} \tag{6}$$

The subscripts 1, 2 and F indicate on which space the operators are defined, *i.e.* the Hilbert space of atom 1, of atom 2, and of the radiation field F, respectively. An essential assumption which is made here is that the atoms are not interacting simultaneously with the same field, *i.e.*, $\Omega(t)\Omega(t-T) \approx 0$, where T is the distance in time of the two atoms (see Fig. 1). The phases λ_1 and λ_2 are related by the equation

$$\lambda_2 = \lambda_1 + \Delta T, \tag{7}$$

since the phase of the field in C changes during the delay time T relative to the second atom. The value of λ_1 is of no relevance.

The operators $b^\dagger$, b denote the creation and annihilation operators of the field mode and the atomic operators are defined by

$$\sigma_k = |g,k\rangle\langle e,k|,$$

where $k = 1, 2$ indicates again the space on which these operators are defined (in the following we omit the label k in state vectors). The environment is modeled as a collection of harmonic oscillators which interact with the field mode *via* amplitude coupling. It is assumed here that the center of mass motion of an atom can be described by a classical uniform motion $r(t) = r_0 + vt$ leading to a time dependent coupling function $\Omega(t)$. This assumption is justified since the kinetic energy of an atom is much larger than the height and the depth of the optical potential given by the eigenenergies of the Hamiltonian (6) using the coupling function (1) (see, *e.g.*, [17]).

The dynamics in the resonators R_1 and R_2 is governed by the equation

$$\dot\rho_{\rm 12F}(t) = \left(\mathcal{J}_k + \mathcal{L}_{\rm F}\right)\rho_{\rm 12F}(t) \tag{8}$$

with

$$\mathcal{J}_k\rho_{\rm 12F}(t) = -\frac{\rm i}{\hbar}\left[V_k, \rho_{\rm 12F}(t)\right], \tag{9}$$

and

$$V_k = -\frac{\hbar\Omega_{\rm R}}{2}\left({\rm e}^{{\rm i}(\varphi_0+\epsilon_k)}\sigma_k + {\rm e}^{-{\rm i}(\varphi_0+\epsilon_k)}\sigma_k^\dagger\right), \tag{10}$$

that is, with an appropriate choice of the Rabi frequency $\Omega_{\rm R}$ the atoms undergo a $\pi/2$ pulse. The phase φ_0 is set equal to zero for R_1 and is given by $\varphi_0 = (\omega_{\rm R} - \omega)\delta t$ when the atom crosses R_2, where δt is the separation of the $\pi/2$-pulses for an atom, *i.e.* the time of flight between R_1 and R_2 (about 230 μs in the experiment). As above it is assumed that the atoms do not interact with the field in one of these resonators at the same time. In analogy to equation (7) the phases ϵ_1 and ϵ_2 are related by

$$\epsilon_2 = \epsilon_1 + (\omega_{\rm R} - \omega)T, \tag{11}$$

$$\tilde{\rho}_{12\mathrm{F}}(T+\tau_\mathrm{C}) = \underbrace{\overbrace{\mathrm{e}^{\mathcal{J}_2\tau_\mathrm{R}}}^{\substack{R_2\\ \text{Atom 2}}}\ \overbrace{\mathcal{M}_{2\mathrm{F}}(\tau_\mathrm{C})}^{\substack{C\\ \text{Atom 2}}}\ \overbrace{\rho_2}^{\substack{R_1\\ \text{Atom 2}}}}_{\substack{\text{“Probing” the}\\ \text{Schrödinger–Cat}\\ \text{by atom 2}}}\ \underbrace{\mathrm{e}^{\mathcal{L}_\mathrm{F}(T-\tau_\mathrm{C})}}_{\substack{\text{Field-}\\ \text{damping}}}\ \underbrace{P_1\{\ \overbrace{\mathrm{e}^{\mathcal{J}_1\tau_\mathrm{R}}}^{\substack{R_2\\ \text{Atom 1}}}\ \overbrace{\mathcal{M}_{1\mathrm{F}}(\tau_\mathrm{C})\,\rho_\mathrm{F}}^{\substack{C\\ \text{Atom 1}}}\ \overbrace{\rho_1}^{\substack{R_1\\ \text{Atom 1}}}\ \}P_1}_{\substack{\text{Preparation of the}\\ \text{Schrödinger–Cat}\\ \text{by atom 1}}} \tag{16}$$

where ϵ_1 may be chosen arbitrarily.

Consider now a pair of atoms which traverses the cavities (see Fig. 1). After excitation in the circular Rydberg state and after the first $\pi/2$-pulse in R_1 the atoms are prepared in the state $(|e\rangle + |g\rangle)/\sqrt{2}$, while the field in the central cavity is in a coherent state $|\alpha\rangle$. For the sake of simplicity we will assume in the following discussion that the distance of the atoms is smaller than the distance of R_1 and C or of C and R_2 or of R_2 and D_e, D_g. However, the distance will be assumed to be still large enough to avoid a simultaneous interaction of both atoms with one of the fields. In the case of a larger delay between the atoms the discussion is completely analogous. Denoting the initial state by $\rho_{12\mathrm{F}} = \rho_1\rho_2\rho_\mathrm{F}$ the time evolution of the complete system until the detection of the second atom reads

$$\begin{aligned} P_2\Big\{&(\mathbf{1}_1\mathbf{1}_2\mathrm{e}^{\mathcal{L}_\mathrm{F}T})P_1\Big[(\mathbf{1}_1\mathbf{1}_2\mathrm{e}^{\mathcal{L}_\mathrm{F}(\tau_\mathrm{RD}-T)})(\mathbf{1}_1\mathrm{e}^{(\mathcal{J}_2+\mathcal{L}_\mathrm{F})\tau_\mathrm{R}})\\ &\times(\mathbf{1}_1\mathbf{1}_2\mathrm{e}^{\mathcal{L}_\mathrm{F}(T-\tau_\mathrm{R})})(\mathrm{e}^{(\mathcal{J}_1+\mathcal{L}_\mathrm{F})\tau_\mathrm{R}}\mathbf{1}_2)(\mathbf{1}_1\mathbf{1}_2\mathrm{e}^{\mathcal{L}_\mathrm{F}(\tau_\mathrm{CR}-T)})\\ &\times(\mathbf{1}_1\mathcal{M}_{2\mathrm{F}}(\tau_\mathrm{C}))(\mathbf{1}_1\mathbf{1}_2\mathrm{e}^{\mathcal{L}_\mathrm{F}(T-\tau_\mathrm{C})})(\mathcal{M}_{1\mathrm{F}}(\tau_\mathrm{C})\mathbf{1}_2)(\rho_1\rho_2\rho_\mathrm{F})\Big]P_1\Big\}P_2, \end{aligned} \tag{12}$$

where $\mathbf{1}_1$ and $\mathbf{1}_2$ denote the identity operators in $\mathcal{H}_{\mathrm{A}_1}$ and $\mathcal{H}_{\mathrm{A}_2}$, respectively. The quantity

$$\mathcal{M}_{k\mathrm{F}}(t)\rho_{12\mathrm{F}} \tag{13}$$

denotes the solution of equation (4) and P_1 and P_2 are the projections on the ground or on the excited state of the atoms, representing the measurements in the detectors D_e and D_g. For the definition of the time intervals τ_R, τ_C, τ_CR and τ_RD, see Figure 1.

It is immediately clear that

$$[\mathcal{J}_k, \mathcal{L}_\mathrm{F}] = 0, \tag{14}$$

since these superoperators act on different spaces. Analogous conditions are fulfilled for the projection operators and $\mathcal{L}_\mathrm{F}$ and for the projection operators among themselves. Using this fact we are now able to change the order of expression (12) which yields

$$P_2\Big\{\mathrm{e}^{\mathcal{L}_\mathrm{F}(\tau_\mathrm{RD}+\tau_\mathrm{R}+\tau_\mathrm{CR})}\tilde{\rho}_{12\mathrm{F}}(T+\tau_\mathrm{C})\Big\}P_2, \tag{15}$$

where the density operator at time $T+\tau_\mathrm{C}$ is given by

see equation (16) above.

For simplicity the identity operators are omitted here. This expression allows an interpretation of the experiment in a new way: the first atom prepares a superposition of two mesoscopic field states. Then, after a delay $T-\tau_\mathrm{C}$, a second atom “probes” the field, *i.e.* the decoherence. If we further assume that $\tau_\mathrm{C} \ll T$ or, to be more precise if

$$\mathcal{M}_{k\mathrm{F}}(\tau_\mathrm{C}) \approx \mathrm{e}^{\mathcal{L}_\mathrm{F}\tau_\mathrm{C}}\mathcal{M}'_{k\mathrm{F}}(\tau_\mathrm{C}), \tag{17}$$

where $\mathcal{M}'_{k\mathrm{F}}(t)\rho_{12\mathrm{F}}(0)$ is the solution of equation (4) with $\gamma = 0$, the chronology of the experiment would be exactly the same as it is proposed in [18]. The damping part in equation (15) does not have any effect on the measured quantities since the generator $\mathcal{L}_\mathrm{F}$ conserves the trace (see [19] for details).

3.2 Approximative model

For the sake of completeness we give a short summary of the basic steps which yield an approximative description of the evolution of the system under consideration which has an analytical solution. To this end, we will interpret the evolution according to equation (16) and make use of the essential condition (17), *i.e.*, we neglect the coupling of the field to the environment during the atom-field interaction.

As already mentioned, each atom undergoes a first $\pi/2$-pulse in the resonator R_1 preparing the state into

$$\frac{1}{\sqrt{2}}\left(|e\rangle + |g\rangle\right). \tag{18}$$

The interaction of the coherent field in the high-Q cavity C with an atom can be described by the unitary transformation

$$\begin{aligned} |e\rangle|\alpha\rangle &\xrightarrow{\ C\ } \mathrm{e}^{\mathrm{i}\phi}|e\rangle|\alpha\mathrm{e}^{\mathrm{i}\phi}\rangle,\\ |g\rangle|\alpha\rangle &\xrightarrow{\ C\ } |g\rangle|\alpha\mathrm{e}^{-\mathrm{i}\phi}\rangle. \end{aligned} \tag{19}$$

The initial superposition (18) is thus transformed into the entangled state

$$\frac{1}{\sqrt{2}}\left(\mathrm{e}^{\mathrm{i}\phi}|e,\alpha\mathrm{e}^{\mathrm{i}\phi}\rangle + |g,\alpha\mathrm{e}^{-\mathrm{i}\phi}\rangle\right). \tag{20}$$

This is a superposition of two mesoscopic field states, often denoted as Schrödinger cat.

The description of the dynamics of the system in this way makes use of several approximations. Basically, the atom-field interaction is described by the first or the second term of Hamiltonian (6). The eigenenergies of this operator in the Schrödinger picture take the form (except for the ground state)

$$E_{\pm,n}(t) = \hbar\nu\left(n+\frac{1}{2}\right) \pm \frac{1}{2}\hbar\Gamma_n(t), \tag{21}$$

with

$$\Gamma_n(t) = \sqrt{\Delta^2 + 4\Omega^2(t)(n+1)}. \tag{22}$$

The corresponding eigenstates $|\pm, n; t\rangle$ are time-dependent dressed states [20], that is, time-dependent linear combinations of the states $|e, n\rangle$ and $|g, n+1\rangle$, where $|n\rangle$ is a Fock state of the field oscillator. Under the condition

$$2\frac{\Omega(r)}{|\Delta|}\sqrt{n+1} \ll 1 \tag{23}$$

the square root in equation (22) can be expanded up to second order which yields

$$\tilde{E}_{\pm,n}(t) = \hbar\nu(n+\frac{1}{2}) \pm \frac{\hbar}{2}|\Delta| \pm \hbar\frac{\Omega^2(t)(n+1)}{|\Delta|}\,. \tag{24}$$

Assuming now that the system is governed by an adiabatic dynamics which holds if the condition

$$\left(\sqrt{\frac{2}{e}}\frac{\Omega_0}{\Delta^2}\frac{v}{w_0}\sqrt{n+1}\right)^2 \ll 1 \tag{25}$$

is fulfilled, the time evolution of an eigenstate can be described with the help of the adiabatic theorem [21], which means that the time-evolution operator $U(t, t_0)$ can be approximated by

$$U(t,t_0)|\pm, n; t_0\rangle = \exp\left(-\frac{\mathrm{i}}{\hbar}\int_{t_0}^{t}\tilde{E}_{\pm,n}(\tau)\mathrm{d}\tau\right)|\pm, n; t\rangle. \tag{26}$$

If we further assume that at times t_0 and t the atom is outside the cavity, *i.e.* $r(t_0) \ll w_0$ and $r(t) \gg w_0$, and, hence, $\Omega(t_0) \approx 0$ and $\Omega(t) \approx 0$, the time evolution of an eigenstate in the interaction picture is given by

$$U_{\mathrm{I}}(t,t_0)|e,n\rangle = \mathrm{e}^{\mathrm{i}\phi(n+1)}|e,n\rangle, \tag{27a}$$
$$U_{\mathrm{I}}(t,t_0)|g,n\rangle = \mathrm{e}^{-\mathrm{i}\phi n}|g,n\rangle, \tag{27b}$$

where the phase ϕ takes the form

$$\phi = -\frac{\Omega_0^2}{\Delta}t_{ww}, \tag{28}$$

with an effective interaction time

$$t_{ww} = \int_{-\infty}^{\infty}\mathrm{d}t\,\frac{\Omega^2(t)}{\Omega_0^2} = \sqrt{\frac{\pi}{2}}\frac{w_0}{v}\,. \tag{29}$$

Applying the evolution operator (27) to the initial state $(|e,\alpha\rangle + |g,\alpha\rangle)/\sqrt{2}$ yields the Schrödinger cat state (20).

It should be kept in mind that this description is justified only if conditions (23, 25) are fulfilled. While condition (25) is well-satisfied for the experimental parameters used in reference [6], condition (23) is, in general, not: for example, using a detuning of 70 kHz and a mean photon number of $|\alpha|^2 = 3.3$ (see below), the left-hand side of inequality (23) is found to be of the order 1. Furthermore, it is essential for the validity of the approximate model that the coherent dynamics dominates and that relaxation processes can be neglected during the atom-field interaction time t_{int}, *i.e.*,

$$\Omega_0, \frac{1}{t_{\mathrm{int}}} \gg \gamma_{\mathrm{at}}, \gamma, \tag{30}$$

which is often denoted as a strong coupling and high-Q regime. However, it should be emphasized here that the time scale $1/\gamma$ characterizes the *relaxation time* of the system. In contrast to this, the *decoherence time* is often much smaller and the question arises if it is justified to neglect this effect during the atom-field interaction.

The first atom is now subjected to the second $\pi/2$-pulse in R_2 and is finally detected in D_{e} or D_{g}. Depending on the result of the measurement one gets one of the field states

$$\frac{1}{\sqrt{N(\chi)}}\left(|\alpha\mathrm{e}^{-\mathrm{i}\phi}\rangle + \mathrm{e}^{\mathrm{i}\xi}|\alpha\mathrm{e}^{\mathrm{i}\phi}\rangle\right), \tag{31}$$

where $N(\chi)$ is a normalization factor and $\xi = \chi + \varphi_0 + \phi$, with $\chi = \pi$ if the atom was found in the ground state, and $\chi = 0$ if the atom was found in the excited state. It should be stressed that in the actual experiment these states, which are also often referred to as Schrödinger cats, never appear but the evolution can be interpreted in a way *as if* one of these states would exist.

The subsequent dynamics of the field is governed by the equation

$$\dot{\rho}_{\mathrm{F}} = \mathcal{L}_{\mathrm{F}}\rho_{\mathrm{F}}, \tag{32}$$

which has the solution [22]

$$\begin{aligned}\rho_{\mathrm{F}}(T;\chi) = \frac{1}{N(\chi)}\Big\{&|\alpha\mathrm{e}^{\mathrm{i}\phi}\mathrm{e}^{-\frac{\gamma}{2}T}\rangle\langle\alpha\mathrm{e}^{\mathrm{i}\phi}\mathrm{e}^{-\frac{\gamma}{2}T}| \\ &+|\alpha\mathrm{e}^{-\mathrm{i}\phi}\mathrm{e}^{-\frac{\gamma}{2}T}\rangle\langle\alpha\mathrm{e}^{-\mathrm{i}\phi}\mathrm{e}^{-\frac{\gamma}{2}T}| \\ &+\Gamma(T)\mathrm{e}^{\mathrm{i}\xi}|\alpha\mathrm{e}^{\mathrm{i}\phi}\mathrm{e}^{-\frac{\gamma}{2}T}\rangle\langle\alpha\mathrm{e}^{-\mathrm{i}\phi}\mathrm{e}^{-\frac{\gamma}{2}T}| \\ &+\Gamma^*(T)\mathrm{e}^{-\mathrm{i}\xi}|\alpha\mathrm{e}^{-\mathrm{i}\phi}\mathrm{e}^{-\frac{\gamma}{2}T}\rangle\langle\alpha\mathrm{e}^{\mathrm{i}\phi}\mathrm{e}^{-\frac{\gamma}{2}T}|\Big\},\end{aligned} \tag{33}$$

where $\Gamma(T)$ is given by

$$\Gamma(T) = \mathrm{e}^{-|\alpha|^2(1-\mathrm{e}^{2\mathrm{i}\phi})(1-\mathrm{e}^{-\gamma T})}. \tag{34}$$

This quantity and, therefore, the off-diagonal terms of the density operator (33) vanish in the case of sufficiently large $|\alpha|^2$ and phase ϕ on a small time scale

$$t_{\mathrm{D}} = \frac{1}{2\gamma|\alpha|^2\sin^2\phi} \ll 1/\gamma, \tag{35}$$

leading to the decoherence of the initial superposition (31).

After a delay time T the second atom traverses the apparatus. Taking (33) as initial state of the field the dynamics of the system can be described in exactly the same way as for the first atom. Thus, it is possible to calculate an analytical expression for the quantity

$$\eta(T;\varphi_0) = W_{\mathrm{ee}}(T;\varphi_0) - W_{\mathrm{ge}}(T;\varphi_0), \tag{36}$$

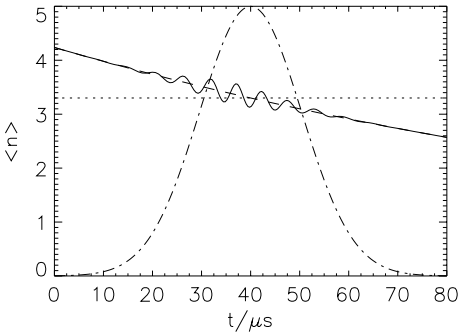

Fig. 3. Plot of the numerically calculated mean photon number $\langle n(t)\rangle = \mathrm{Tr}\left\{\rho_{1\mathrm{F}}(t)b^\dagger b\right\}$ (solid line) during interaction of atom and field for $\Delta/2\pi = 170$ kHz with an initial photon number of 4.2. The dashed line corresponds to $4.2\mathrm{e}^{-t/T_\mathrm{R}}$, the horizontal (dotted) line to a constant value of 3.3, and the dashed-dotted line is proportional to the atom-field coupling function $\Omega(t)$.

which is measured in the experiment [15]. Taking the average over φ_0 one can show, employing certain conditions which are fulfilled for the experimental parameters, that

$$\bar{\eta}(T) = \frac{1}{2\pi}\int_0^{2\pi} \mathrm{d}\varphi_0\, \eta(T;\varphi_0) \approx \frac{1}{2}\mathrm{Re}\left\{\Gamma(T)\right\}\cdot \qquad (37)$$

Therefore, $\bar{\eta}(T)$ is a direct measure for the decoherence of the state (31).

As already mentioned the state (31) does not exist in the experiment in this form. By contrast, the state (20) does exist (at least within the framework of this approximative model). Taking (20) as initial state, equation (32) can be solved, too, leading to the same decoherence behaviour, *i.e.* the off-diagonal elements of the resulting density matrix vanish on the same time scale. Hence, from this point of view it does not matter which state exists in reality and both pictures are equivalent.

4 Results of simulations and discussion

In this section we present and discuss the results of some simulations of the atom-field system according to the exact model presented in Section 3.1. To this end, equation (4) is solved numerically. This means that we take into account the damping of the field mode during the atom-field interaction. Moreover, the approximations of the analytically solvable model, which are not very well-satisfied for the experimental parameters used, are avoided in this way. The only important approximation underlying our model is the treatment of the center of mass dynamics of the atoms as a given uniform classical motion.

The choice of initial conditions for our simulations is illustrated in Figure 3 which shows a plot of the mean photon number $\langle n(t)\rangle$ of the field in C during the passage of an atom as a function of time. In the experiment the mean photon number is measured to be approximately $\langle n(t_\mathrm{C})\rangle \approx 3.3$ roughly at the time t_C when the first atom is at cavity center (*i.e.* $t_\mathrm{C} = 40\,\mu$s in Fig. 3). The interaction time τ_C is taken to be $80\,\mu$s (see Fig. 1). Thus, we start our simulation at time $t = 0$, that is at $t_\mathrm{C} - 40\,\mu$s, when the atom-field coupling is practically zero. As can be seen from Figure 3 the initial photon number is then approximately

$$\langle n(0)\rangle = \langle n(t_\mathrm{C})\rangle \mathrm{e}^{40\,\mu\mathrm{s}/T_\mathrm{R}} \approx 4.2, \qquad (38)$$

where $T_\mathrm{R} = 160\,\mu$s is the actual mean photon lifetime of the cavity [6] if field damping is taken into account. Thus, we take the initial condition $\alpha^2 = 4.2$ in all cases in which $\gamma \neq 0$. If field damping is neglected, that is in those cases in which we set $\gamma = 0$ during atom-field interaction, we take the initial condition $\alpha^2 = 3.3$ corresponding to the mean photon number when the atom crosses the cavity center.

4.1 State of the field after preparation of the Schrödinger cat

The first quantity under consideration is the state of the field according to the scheme (16). In particular, we will examine the state of the field after the preparation of the Schrödinger cat, *i.e.* the field component of the state

$$P_1\left\{\mathrm{e}^{\mathcal{J}_1\tau_\mathrm{R}}\mathcal{M}_{1\mathrm{F}}(\tau_\mathrm{C})\rho_1\rho_\mathrm{F}\right\}P_1 \qquad (39)$$

in the Wigner representation [23,24]. The results of the simulation with $\Delta/2\pi = 70$ kHz for vanishing and for a finite field-environment coupling are shown in Figures 4 and 5. As it can be seen the initial state $|\alpha\rangle$ evolved into a superposition of two nearly separated field components in phase space which have approximately the shape of coherent states. However, the magnitude of the phase is about $\phi \approx 0.7$ which is smaller than predicted by the approximative model. Here, the phase has a value close to $\phi \approx 1$. This discrepancy is explained by the fact that condition (23) is merely insufficiently fulfilled and was already mentioned in [15]. Furthermore, due to field damping, a reduction of the interferences has taken place already after the interaction time. This phenomenon, *i.e.* decoherence *during* the preparation of the superposition, will be examined in Sections 4.3 and 4.4.

Figures 6 and 7 show the analogous graphs for $\Delta/2\pi = 170$ kHz. In this case one expects a better legitimation of condition (23). However, the overlap of the two field components is much larger than in the case of the smaller detuning. Nevertheless it is clearly realizable that the negative parts of the Wigner function are significantly reduced due to the coupling of the field to the environment.

4.2 The difference between the conditional probabilities

Now the question arises of whether the effects outlined in the previous section have any consequences on the difference of the conditional probabilities, *i.e.* on the quantity which was actually measured in the experiment. For the purpose of a numerical simulation one can use the time

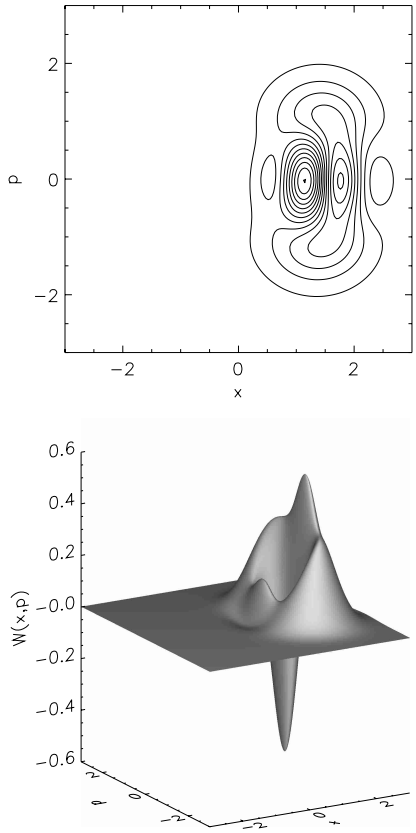

Fig. 4. Wigner function of the field state after preparation as contour plot and as three dimensional plot for $\Delta/2\pi = 70\,\mathrm{kHz}$, $\varphi_0 = 0$ and $\gamma = 0$. The phase of the initial state was supposed to be zero ($\alpha^2 = 3.3$).

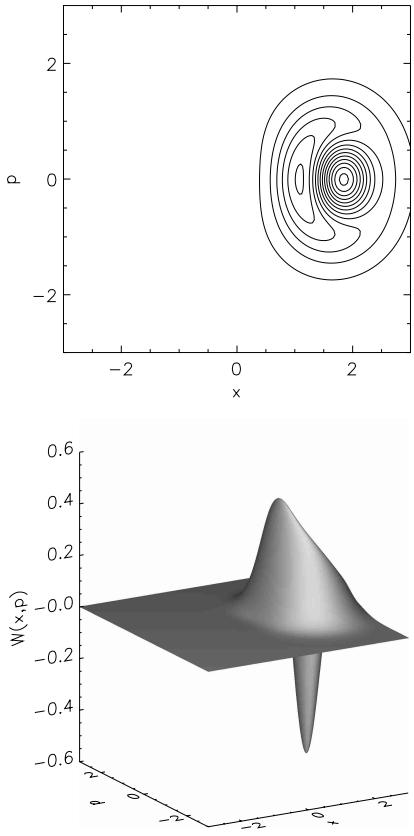

Fig. 6. Wigner function of the field state after preparation corresponding to Figure 4 for $\Delta/2\pi = 170\,\mathrm{kHz}$, $\gamma = 0$ and $\alpha^2 = 3.3$.

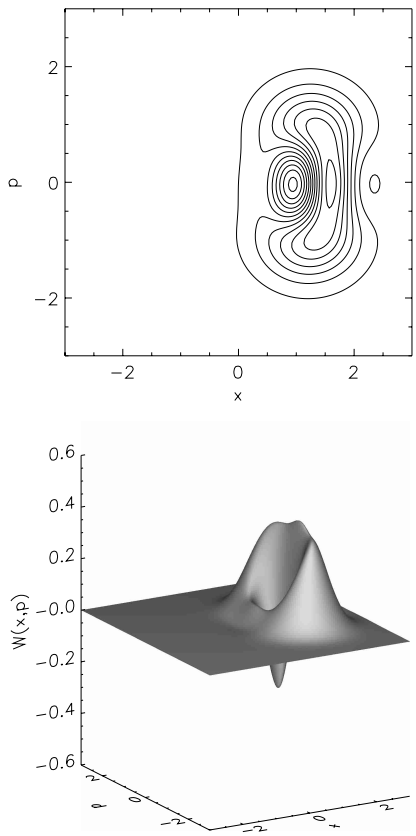

Fig. 5. Wigner function of the field state after preparation corresponding to Figure 4 for $\Delta/2\pi = 70\,\mathrm{kHz}$, $\gamma = 1/T_\mathrm{R}$ and $\alpha^2 = 4.2$.

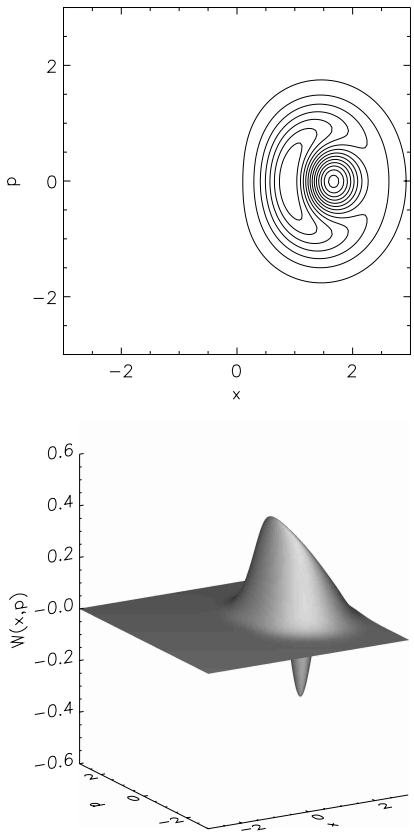

Fig. 7. Wigner function of the field state after preparation corresponding to Figure 5 for $\Delta/2\pi = 170\,\mathrm{kHz}$, $\gamma = 1/T_\mathrm{R}$ and $\alpha^2 = 4.2$.

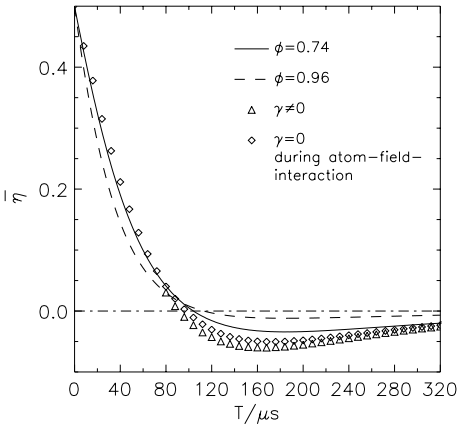

Fig. 8. Mean of the difference of the conditional probabilities $\bar{\eta}$ for $\Delta/2\pi = 70\,\mathrm{kHz}$.

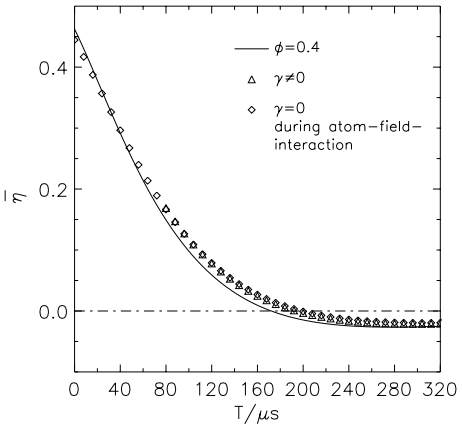

Fig. 9. Mean of the difference of the conditional probabilities $\bar{\eta}$ for $\Delta/2\pi = 170\,\mathrm{kHz}$.

evolution as it is described by equation (16) or by the real evolution (12). However, the first one is much easier to implement. The results are displayed in Figures 8 and 9 where we used once again the parameters of the experiment. The solid lines correspond to the analytical solution. In Figure 8 this analytical solution is determined for a phase $\phi = 0.74$ (like in [6,15]) in order to take into account the effects mentioned in Section 4.1 (in contrast to Eq. (28), which would lead to an angle $\phi \approx 1$, see dashed line in Fig. 8), while in Figure 9 the phase was calculated according to equation (28). It should be emphasized here that these lines are exactly the same ones as in Figure 5 of [6], apart from a scaling factor of 0.36 applied to the y-axis which takes into account some experimental imperfections. The diamonds correspond to the case $\gamma = 0$, *i.e.* relation (17). The triangles are the simulation results for $\gamma \neq 0$. Note that in this case the minimal delay time is taken to be $\tau_C = 80\,\mu$s. Of course it could be interesting both experimentally and theoretically to investigate in detail the range of smaller delays, in which case two atoms are simultaneously in the cavity.

According to Figures 8 and 9 there is a relatively good agreement between the simulations and the analytically calculated lines and, therefore, also with the experimental data. In case of $\gamma = 0$ the (small) deviations to the analytical lines are due to the approximations made in the description of the Jaynes-Cummings dynamics (see Sect. 3.2), whereas the effect of approximation (17) leads to the difference between diamonds and triangles (see also the related discussion in Sect. 4.4). The conclusion is that the quantity $\bar{\eta}$ is described by the analytical model to a sufficient degree of accuracy, especially if one compares it with the data gained from the experiment (which has of course a finite accuracy). However this does not imply that any quantity is satisfactorily reproduced by the analytical model. We are therefore going to take a closer look now at more sensitive quantities, in particular those describing decoherence effects during the preparation process.

4.3 Decoherence time and preparation time

In order to examine the effect of decoherence during the preparation process we consider a single atom which interacts with the field in C, *i.e.* the process

$$\mathcal{M}_{1\mathrm{F}}(t)\rho_1\rho_\mathrm{F}, \tag{40}$$

where $\rho_1\rho_\mathrm{F}$ is the state of the atom-field system right before the atom enters the central cavity,

$$\rho_1\rho_\mathrm{F} = \frac{1}{2}\big(|e\rangle\langle e| + |g\rangle\langle g| + |e\rangle\langle g| + |g\rangle\langle e|\big)|\alpha\rangle\langle\alpha|. \tag{41}$$

If one makes use of equation (17) and the approximations mentioned in Section 3.2, the state would then be prepared into the entangled cat state (20)

$$\begin{aligned}\rho_{1\mathrm{F}} = \frac{1}{2}\big(&|e,\alpha\mathrm{e}^{\mathrm{i}\phi}\rangle\langle e,\alpha\mathrm{e}^{\mathrm{i}\phi}| + |g,\alpha\mathrm{e}^{-\mathrm{i}\phi}\rangle\langle g,\alpha\mathrm{e}^{-\mathrm{i}\phi}| \\ &+ \mathrm{e}^{\mathrm{i}\phi}|e,\alpha\mathrm{e}^{\mathrm{i}\phi}\rangle\langle g,\alpha\mathrm{e}^{-\mathrm{i}\phi}| + \mathrm{e}^{-\mathrm{i}\phi}|g,\alpha\mathrm{e}^{-\mathrm{i}\phi}\rangle\langle e,\alpha\mathrm{e}^{\mathrm{i}\phi}|\big)\end{aligned} \tag{42}$$

and *then* evolves according to equation (32) which yields

$$\begin{aligned}\rho_{1\mathrm{F}}(t) = \frac{1}{2}\Big\{&|e,\alpha\mathrm{e}^{\mathrm{i}\phi}\mathrm{e}^{-\frac{\gamma}{2}t}\rangle\langle e,\alpha\mathrm{e}^{\mathrm{i}\phi}\mathrm{e}^{-\frac{\gamma}{2}t}| \\ &+ |g,\alpha\mathrm{e}^{-\mathrm{i}\phi}\mathrm{e}^{-\frac{\gamma}{2}t}\rangle\langle g,\alpha\mathrm{e}^{-\mathrm{i}\phi}\mathrm{e}^{-\frac{\gamma}{2}t}| \\ &+ \Gamma(t)\mathrm{e}^{\mathrm{i}\phi}|e,\alpha\mathrm{e}^{\mathrm{i}\phi}\mathrm{e}^{-\frac{\gamma}{2}t}\rangle\langle g,\alpha\mathrm{e}^{-\mathrm{i}\phi}\mathrm{e}^{-\frac{\gamma}{2}t}| \\ &+ \Gamma^*(t)\mathrm{e}^{-\mathrm{i}\phi}|g,\alpha\mathrm{e}^{-\mathrm{i}\phi}\mathrm{e}^{-\frac{\gamma}{2}t}\rangle\langle e,\alpha\mathrm{e}^{\mathrm{i}\phi}\mathrm{e}^{-\frac{\gamma}{2}t}|\Big\},\end{aligned} \tag{43}$$

where $\Gamma(t)$ is given by equation (34). Obviously, the initial state (41) changes into a statistical mixture on a time scale given by $\Gamma(t)$, *i.e.* in this picture the system evolves first into the (pure) superposition and then decoherence takes place. In order to quantify this transition one can use $\mathrm{Tr}\{\rho_{1\mathrm{F}}^2\}$ which represents a measure of the "purity" of a state (often the idempotency defect of linear entropy $1 - \mathrm{Tr}\{\rho_{1\mathrm{F}}^2\}$ is used as well [25]). In the case of expression (43) this quantity can easily be calculated and is given by

$$\begin{aligned}\mathrm{Tr}\left\{\rho_{1\mathrm{F}}^2(t)\right\} &= \frac{1}{2}\left(1 + |\Gamma(t)|^2\right) \\ &= \frac{1}{2}\left(1 + \mathrm{e}^{-4|\alpha|^2\sin(\phi)^2(1-\mathrm{e}^{-\gamma t})}\right),\end{aligned} \tag{44}$$

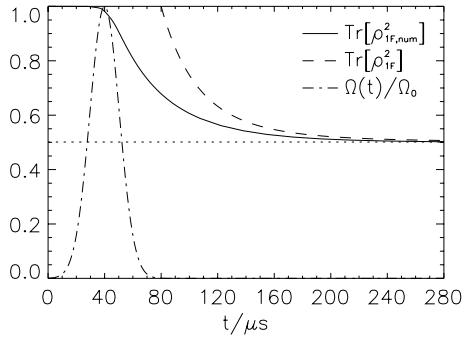

Fig. 10. Demonstration of the transition from the pure state to a statistical mixture using the "purity" $\mathrm{Tr}\{\rho_{1\mathrm{F}}^2\}$. The solid line corresponds to a numerical calculation, the dashed line to equation (44) and the horizontal line represents its asymptotic value. The dashed-dotted line is the time dependent coupling function (normalized to one). The parameters are $\Delta/2\pi = 70\,\mathrm{kHz}$, $|\alpha|^2 = 3.3$ ($|\alpha|^2 = 4.2$ for the solid line), $T_\mathrm{R} = 160\,\mu\mathrm{s}$ and $\phi = 0.74$ (for the analytical line).

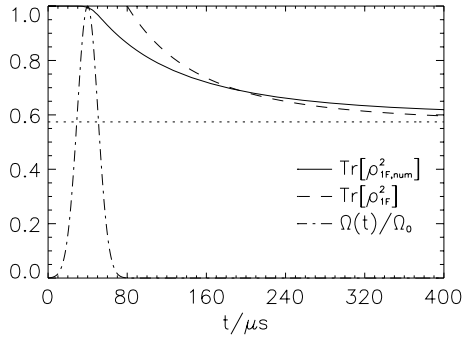

Fig. 11. Purity of the field state corresponding to Figure 10 for $\Delta/2\pi = 170\,\mathrm{kHz}$. In case of the analytical curve the phase ϕ is set to 0.4.

which is a monotonously decreasing function of t with the asymptotic value

$$\mathrm{Tr}\left\{\rho_{1\mathrm{F}}^2(\infty)\right\} = \frac{1}{2}\left(1 + \mathrm{e}^{-4|\alpha|^2\sin(\phi)^2}\right). \qquad (45)$$

In studies dealing with decoherence it is sometimes implicitly assumed that decoherence takes place only after the completion of the preparation process. Obviously, this is an idealized assumption the validity of which must be investigated. For this purpose the time dependent purity of the atom-field system is displayed in Figures 10 and 11, once again for the experimental parameters. The solid lines correspond to the numerical solution of expression (40) with initial state (41) (at $t = 0$). The dashed-dotted lines represent the time dependent coupling function (normalized to one) and the dashed lines correspond to the analytical expression (44). In the latter case the initial time, *i.e.* the time when the superposition (42) should be prepared is set equal to $t = 80\,\mu\mathrm{s}$, whereas this should be understood only as an estimation since the two models are hardly comparable. Obviously, the initial pure state starts to evolve into a mixture already during the interaction of atom and field, leading to an apparently larger

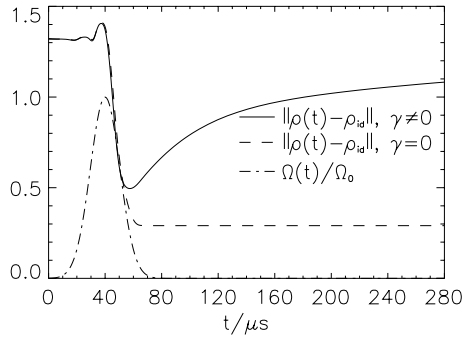

Fig. 12. The "distance" of the numerically calculated density matrix to the ideal state (42) with $\phi = 0.74$. The detuning is $\Delta/2\pi = 70\,\mathrm{kHz}$. The solid line corresponds to a finite atom-field coupling ($T_\mathrm{R} = 160\,\mu\mathrm{s}$) and the dashed line to a vanishing coupling. The other parameters are the same as in Figure 10.

decoherence time. This effect would be even more pronounced if the emerging superposition has a more classical character (*i.e.* in the case of a larger distance of the field components in phase space (*cf.* Figs. 4–7)).

4.4 Hilbert-Schmidt distance to the Schrödinger cat state

Now the question arises to what extent the state of the system coincides with the expected state (42) at all. An appropriate measure for the "distance" of two states is the Hilbert-Schmidt norm which is given by

$$\| A \| \equiv \sqrt{\mathrm{Tr}\,\{A^\dagger A\}}, \qquad (46)$$

where A is an operator. This expression is of course well-defined for density operators since $0 \leq \mathrm{Tr}\{\rho^2\} \leq 1$. Furthermore it is easy to show that the distance of two states fulfills the condition

$$0 \leq \| \rho_1 - \rho_2 \| \leq \sqrt{2} \qquad (47)$$

for arbitrary ρ_1 and ρ_2. We are now interested in the distance of the numerically calculated density matrix $\rho(t) = \rho_{1\mathrm{F,num}}(t)$ to the idealized target state $\rho_\mathrm{id} = \rho_{1\mathrm{F}}$ (Eq. (42)). This distance is a measure for the quality of the approximations made in the analytical model and quantifies to which degree the Schrödinger cat state (20) or (42) is actually prepared.

The results of the simulations are shown in Figures 12 and 13 for the experimental parameters. The solid lines correspond to a calculation with finite field-environment coupling and the dashed lines to a calculation where γ is set equal to zero, whereby the full Jaynes-Cummings Hamiltonian is used. As can be seen from the figures the Hilbert-Schmidt distance does not decrease to zero, neither with nor without field damping. This means that in both cases the idealized Schrödinger cat state (42) is never reached completely. The finite minimal distance of the dashed line ($\gamma = 0$) to the Schrödinger cat can be

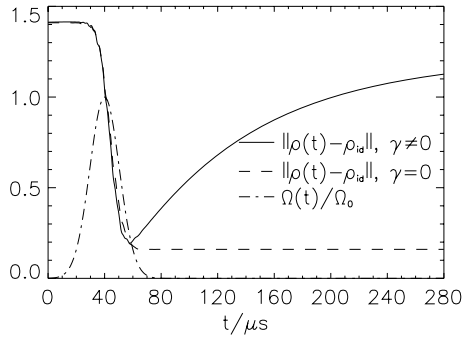

Fig. 13. The "distance" of the numerically calculated density matrix to the ideal state (42) corresponding to Figure 12. The detuning here is $\Delta/2\pi = 170\,\mathrm{kHz}$.

traced back to nonlinearities in the phase shift and to non-adiabatic behaviour of the full Jaynes-Cummings dynamics. Note that the distance to the target state is smaller in the case of the higher detuning since conditions (23, 25) are more justified here. On the other hand, as can be seen from the solid line in Figure 12 a finite field damping ($\gamma \neq 0$) leads to decoherence during the preparation stage of the experiment and, therefore, to a minimal distance to the Schrödinger cat which is larger than for $\gamma = 0$. We also observe that this effect is negligible for the higher detuning (Fig. 13). This could be explained by the fact that in this case the angle between the two phase components of the field is smaller and, thus, the decoherence time becomes larger.

4.5 Conclusion

An important conclusion to be drawn from the example studied in this paper is that, in general, the suppression of quantum coherence must be accounted for already during the initial phase of preparation of the intended target state. As has been demonstrated the analytical model provides a sufficiently accurate description of the experimentally measured quantity, namely the difference $\bar{\eta}$ of conditional probabilities. Nevertheless, the numerical simulations of the complete model revealed that other quantities, such as the Hilbert-Schmidt distance to the target state, show significant deviations from the simple model. One expects that during the preparation of more macroscopic superpositions than the ones discussed in this paper decoherence effects during the preparation phase are strongly enhanced. This fact could lead to important consequences for experimental and theoretical estimations of decoherence times.

References

1. E. Schrödinger, Naturwissenschaften **23**, 807 (1935); 823 (1935); 844 (1935).
2. D. Giulini *et al.*, *Decoherence and the Appearance of a Classical World in Quantum Theory* (Springer, Berlin, 1996).
3. *Relativistic Quantum Measurement and Decoherence*, Vol. 559 of Lecture Notes in Physics, edited by H.P. Breuer, F. Petruccione (Springer, Berlin, 2000).
4. C. Monroe, D.M. Meekhof, B.E. King, D.J. Wineland, Science **272**, 1131 (1996).
5. C.J. Myatt *et al.*, Nature **403**, 269 (2000).
6. M. Brune *et al.*, Phys. Rev. Lett. **77**, 4887 (1996).
7. A.O. Caldeira, A.J. Leggett, Phys. Rev. A **31**, 1059 (1985).
8. W.G. Unruh, W.H. Zurek, Phys. Rev. D **40**, 1071 (1989).
9. W.H. Zurek, Phys. Today **44**, 36 (1991).
10. D. Vitali, P. Tombesi, P. Grangier, Appl. Phys. B **64**, 249 (1997).
11. L. Krippner, W.J. Munro, M.D. Reid, Phys. Rev. A **50**, 4330 (1994).
12. W.J. Munro, M.D. Reid, Phys. Rev. A **52**, 2388 (1995).
13. D.J. Daniel, G.J. Milburn, Phys. Rev. A **39**, 4628 (1989).
14. P. Tombesi, D. Vitali, Phys. Rev. Lett. **77**, 411 (1996).
15. X. Maître *et al.*, J. Mod. Opt. **44**, 2023 (1997).
16. N.F. Ramsey, *Molecular Beams* (Oxford Univ. Press, Oxford, 1985).
17. S. Haroche, J.M. Raimond, in *Cavity Quantum Electrodynamics*, Advances in Atomic, Molecular, and Optical Physics, Suppl. 2, edited by P.R. Berman (Academic Press, New York, 1994), p. 123.
18. L. Davidovich, M. Brune, J.M. Raimond, S. Haroche, Phys. Rev. A **53**, 1295 (1996).
19. U. Dorner, Diploma thesis, University of Freiburg, 2000, available from the authors or at `http://webber.physik.uni-freiburg.de/~dorner`.
20. C. Cohen-Tannoudji, J. Dupont-Roc, G. Grynberg, *Atom-Photon Interactions* (Wiley, New York, 1998).
21. A. Messiah, *Quantum Mechanics* (de Gruyter, Berlin, 1979), Vol. 2.
22. D.F. Walls, G.J. Milburn, Phys. Rev. A **31**, 2403 (1985).
23. W.H. Louisell, *Quantum Statistical Properties of Radiation* (Wiley, New York, 1990).
24. H.J. Carmichael, *Statistical Methods in Quantum Optics* (Springer, Berlin, 1999), Vol. 1.
25. W.H. Zurek, S. Habib, J.P. Paz, Phys. Rev. Lett. **70**, 1187 (1993).